Nuclear Instruments and Methods in Physics Research A 732 (2013) 526–529

Contents lists available at ScienceDirect

Nuclear Instruments and Methods in Physics Research A

journal homepage: www.elsevier.com/locate/nima

Design and characterization of the VMM1 ASIC for micropattern gas detectors

Jessica Metcalfe *, Gianluigi De Geronimo, Jack Fried, Shaorui Li, Neena Nambiar, Venetios Polychronakos, Emerson Vernon

Brookhaven National Laboratory, Upton, NY, USA

ARTICLE INFO

Available online 25 August 2013

Keywords:
ASIC
Micromegas
TGC

ABSTRACT

Measurements of the first prototype VMM1 ASIC designed at Brookhaven National Laboratory in 130 nm CMOS and fabricated in spring 2012 are presented. The 64-channel ASIC features a novel design for use with several types of micropattern gas detectors. The data driven system measures peak amplitude and timing information in tracking mode including sub-threshold neighbors and first channel hit address in trigger mode. Several programmable gain and integration times allows the flexibility to work with Micromegas, Thin Gap Chambers (TGCs), and Gas Electron Multiplier (GEM) detectors. The IC design and features are presented along with measurements characterizing the performance of the VMM1 such as noise, linearity of the response, time walk, and calibration range.

Published by Elsevier B.V.

1. Introduction

The VMM1 ASIC is the first in a series of front-end read-out electronics designed for use with Micromegas and Thin Gap Chambers (TGCs) for ATLAS Upgrade [1–5]. It features a range of gains and peaking times to allow use with other types of micropattern gas detectors as well. It incorporates several innovative features to allow operation in a fast trigger mode in the ATLAS Level 1 trigger as well as in a time projection mode (μ–TPC mode) for precision track reconstruction. The VMM1 features smart token passing reading out only those channels above threshold and their nearest neighbors in order to reduce the bandwidth and increase the potential for new physics.

2. Design

The VMM1 ASIC was fabricated in a commercial 130 nm CMOS process from IBM. It has 64 front-end channels each consisting of low noise charge amplifier (CA), shaper with baseline stabilizer (SA), a discriminator with trimmer (DSC), a peak- and time-detector (PD/TD), a time-to-amplitude converter (TAC), multiplexing with smart token, and direct Time-over-Threshold outputs (TOT) [6] as shown in Fig. 1. A diagram illustrating the signal acquisition is shown in Fig. 2.

2.1. Features

The VMM1 design incorporates many versatile features including flexible gains and peaking times that can be chosen based on different applications. The expected signal on a strip varies depending on the type of gaseous detector, detector capacitance, geometries such as gas gap and strip spacing, and gas amplification properties to name a few examples. The VMM1 can be tuned to optimize signal processing to take advantage of the full measurement range in order to get the most precise measurement values. For example, the simulation of the design performance predicts a charge resolution of approximately 5000e^- for a 25 ns peaking time and 200 pF capacitance and a timing resolution of 1 ns for a 1 V signal amplitude [6]. The following list summarizes the features of the VMM1.

- *Selectable Gain*
  The nominal gain value has the options of 0.5, 1, 3, and 9 mV/fC to accommodate the needs of different applications.
- *Selectable Peaking Time*
  The Peaking Time or integration time can be selected from the following options: 25 ns, 50 ns, 100 ns, and 200 ns.
- *Adjustable TAC slope*
  The time-amplitude-conversion (TAC) slope can be adjusted according to 125 ns/V, 250 ns/V, 500 ns/V and 1 μs/V.
- *Neighbor Readout*
  There is an option to read out the 2 neighboring channels of a channel with a signal over threshold. In the case the neighbor channel is read out by a neighboring VMM1, the information is passed to that ASIC and the neighbor channel signal is acquired.

* Corresponding author. Tel.: +1 41 968 5358.
E-mail addresses: Jessica.Metcalfe@cern.ch, jessica.metcalfe@gmail.com (J. Metcalfe).

0168-9002/$ - see front matter Published by Elsevier B.V.
http://dx.doi.org/10.1016/j.nima.2013.07.092

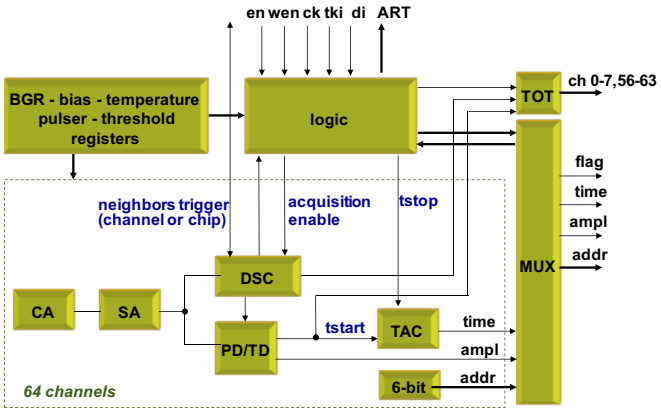

Fig. 1. The block diagram of the first version of the VMM ASIC.

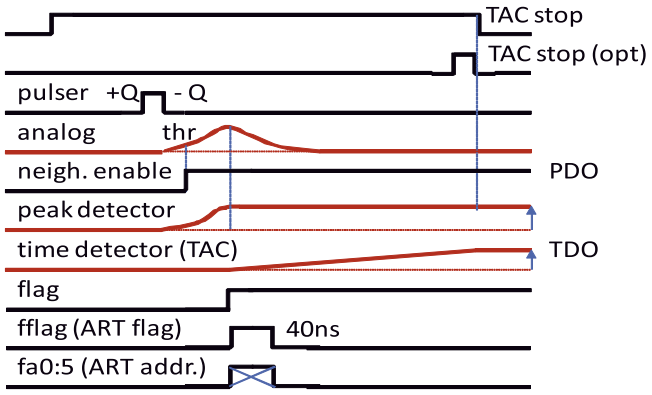

Fig. 2. The acquisition signals of the VMM1. When the signal peak is reached a capacitor begins charging to measure the time since the signal peak was reached and the fast trigger read-out flag is raised and the channel address read out. The PDO and TDO are read out when the TAC stop is lowered.

- *Smart Token Passing*
  This feature allows only the signals above threshold to be read out reducing bandwidth requirements.
- *Fast Trigger Readout*
  The Address in Real Time (ART) reads out the address of the first channel with a signal hit for fast trigger applications.
- *Timing Mode*
  The Time-over-Threshold (ToT) and the Time-to-Peak (TtP) can be read out from dedicated digital outputs for the first and last eight channels.
- *Threshold Trimming*
  The threshold of each channel may be trimmed by approximately 15 mV in order to equalize channel-to-channel variation.
- *Sub-Hysteresis*
  The fast comparator introduces a hysteresis on the threshold of approximately $\pm$10 mV. The Sub-Hysteresis circuit counteracts this by automatically adjusting the threshold level before and after peak detection. (See Sub-Hysteresis section.)

3. Performance

3.1. Peak detection

The peak detector measures with high precision and stores the peak amplitude of the signal in analog memories. The stored amplitudes are then multiplexed to the output called the PDO (Peak Detector Output). For the case where nominal gain=0.5 mV/fC and peaking time=25 ns, and for an input signal of 600 fC the PDO rms is 0.26 mV as shown in Fig. 3.

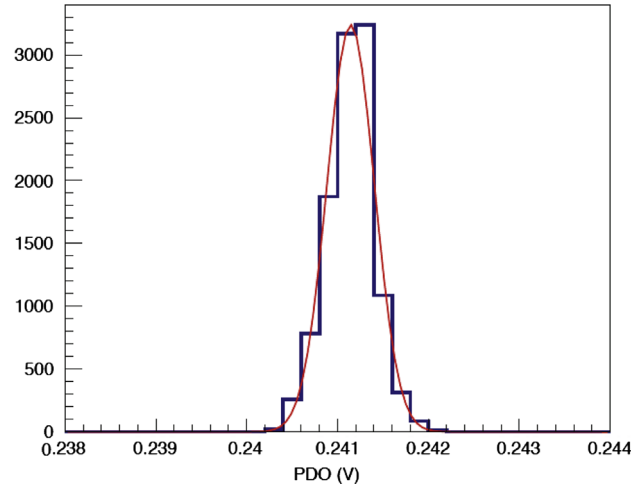

Fig. 3. The response of the PDO for a nominal gain=0.5 mV/fC and peaking time=25 ns, and for an input signal of 600 fC the PDO rms is 0.26 mV.

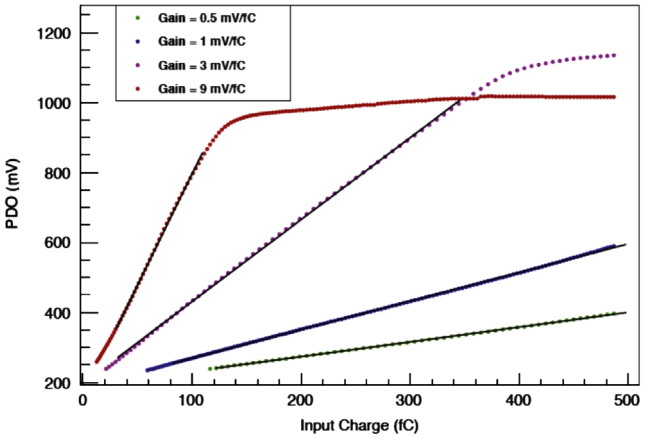

Fig. 4. PDO response as a function of input charge for each of the nominal gain settings and fits to extract measured gains.

There are 4 nominal values each for gain and peaking time. The combination of the configuration determines the real signal gain. Fig. 4 shows the gain linearity for each of the gain settings and demonstrates the range of measurable input charges. Fig. 5 shows the percentage of the linearity error or the percentage error from the expected value from the fit. The linearity error is of the order of less than 0.1%.

3.2. Time detection

The time is measured by charging a capacitor at a specific rate given by the Time-Amplitude-Conversion (TAC) slope from the time the peak is detected until the signal is read out. The TAC slope has several settings to accommodate different applications depending on the signal integration time. In Fig. 6 the TDO response shows a timing resolution of 0.04 ns for nominal gain=0.5 mV/fC, peaking time=25 ns, and TAC=125 ns/V.

The time-walk measures the jitter of the time the peak is detected as the signal amplitude is varied. Ideally, the time is independent of the signal amplitude. The time-walk is shown in Fig. 7 for the VMM1 and is of the order of 1 ns.

3.3. Timing measurements

The first version of the VMM has timing output on 16 channels. There are two modes of operation: Time-over-Threshold (ToT) and

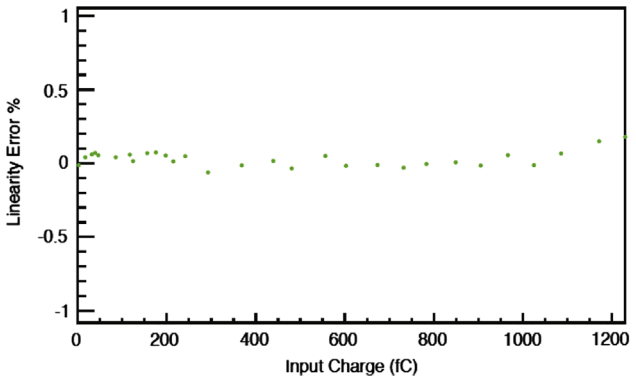

Fig. 5. The percentage linearity error or residual percentage of the PDO response with an external pulser taken at nominal gain of 1 mV/fC and peaking time of 50 ns.

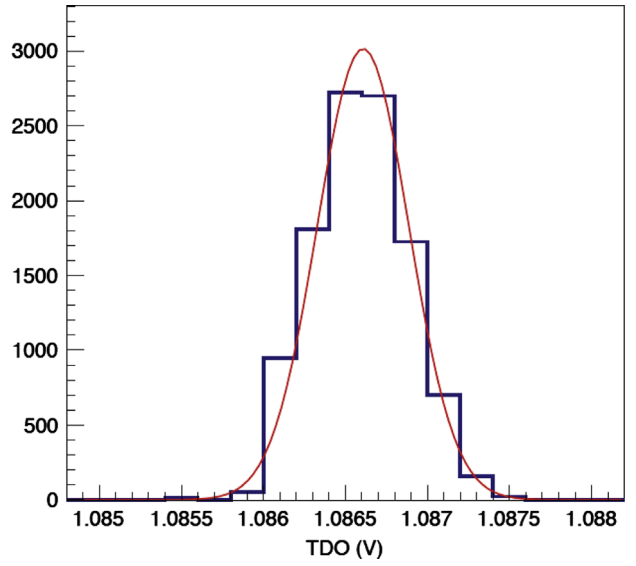

Fig. 6. The response of the TDO for a nominal gain=0.5 mV/fC, peaking time=25 ns, and TAC=125 ns/V. The timing resolution is 0.04 ns.

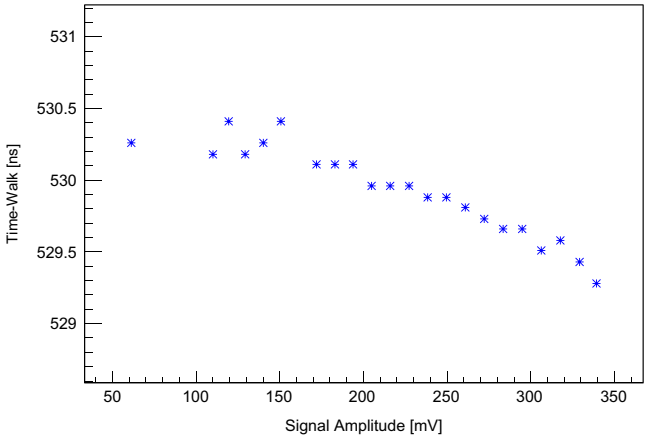

Fig. 7. Time Walk at $g=1$, pT=25 ns shows approximately 1 ns variation over the range of signal amplitudes.

Time-to-Peak (TtP). This feature was designed mainly for use with the TGC detectors. Fig. 8 shows an example of the timing outputs for a signal pulse.

3.4. Threshold

The threshold inherently has some channel-to-channel variation. A threshold trim was included in the VMM1 design to equalize thresholds by allowing each individual channel to be trimmed by approximately 0–15 mV. The threshold was measured by varying the input amplitude and counting the percent of signals that were returned by the acquisition at each input amplitude resulting in an S-curve or turn-on curve. The data points are fit

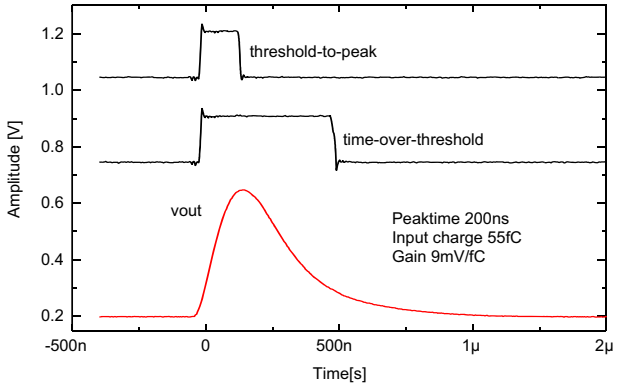

Fig. 8. The timing outputs for ToT and TtP are shown for a signal pulse.

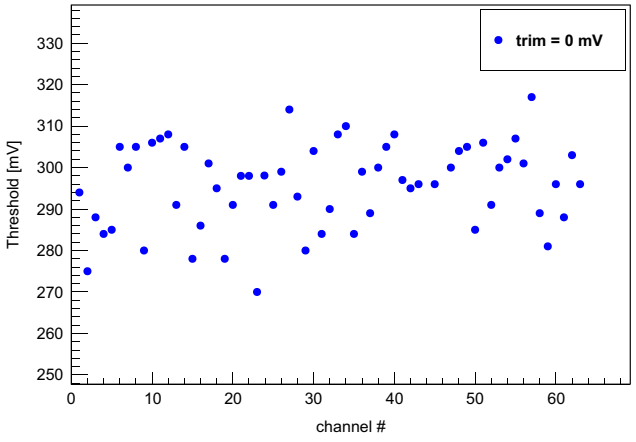

Fig. 9. Thresholds extracted from S-curve measurements versus channel number for the minimum trim setting equal to 0 mV.

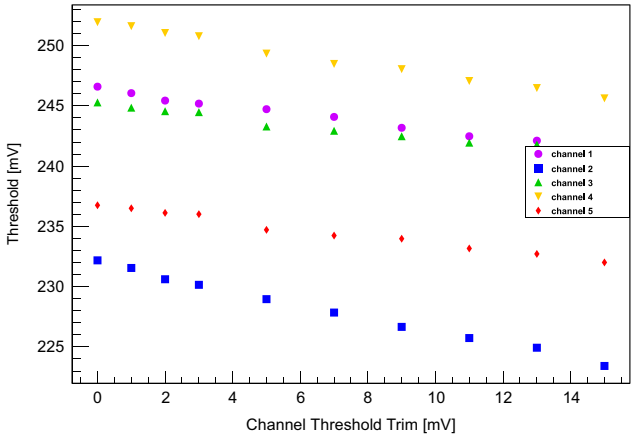

Fig. 10. The trim allowance is shown for the range of programmable trim setting for 5 channels.

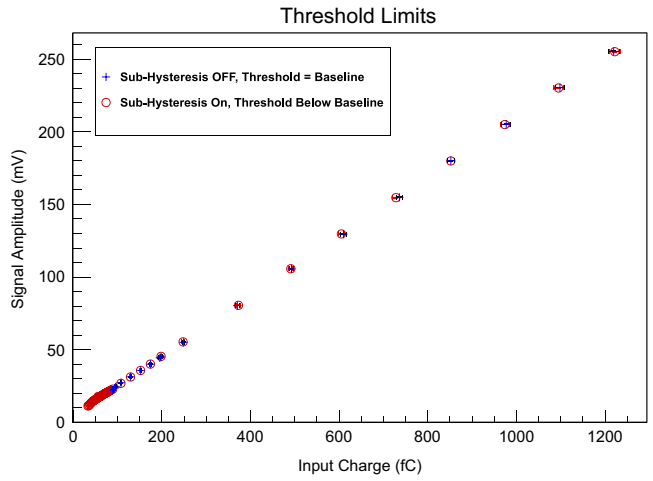

Fig. 11. The lowest threshold setting with and without the Sub-Hysteresis engaged is shown as a function of the input charge. A magnification of the lower region is shown in Fig. 12.

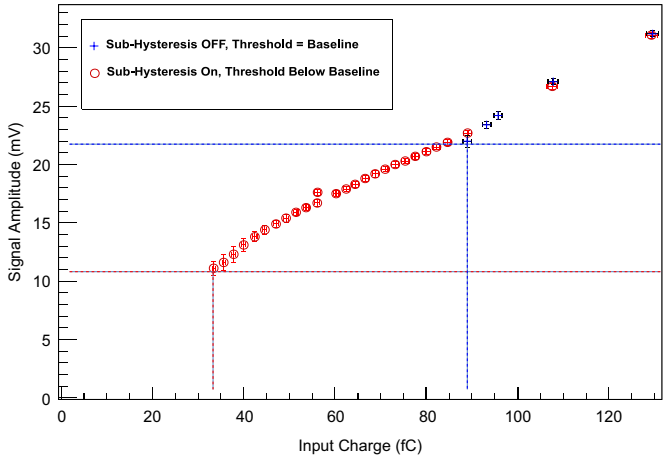

Fig. 12. Fig. 11 is shown again magnified to highlight the Sub-Hysteresis function.

with a Fermi-Dirac function to extract the mid-point of the turn-on (second derivative=0), which gives the threshold for a particular channel. Fig. 9 shows the variation in the threshold channel by channel. Fig. 10 demonstrates the range of the trim for 5 channels. In version 1 of the VMM the trim range is not sufficient to equalize all channels, but will be corrected in the second version.

3.4.1. *Sub-Hysteresis*

The fast comparator introduces a hysteresis, which effectively raises the minimum threshold by approximately ± 10 mV (i.e. a 20 mV window around the nominal threshold). The sub-hysteresis function was introduced to compensate for this effect by moving the threshold level so that it triggers close to the baseline and resets after the peak is detected.

Figs. 11 and 12 show the signal amplitude versus the input charge with and without the sub-hysteresis function for the lowest working threshold. Without the sub-hysteresis function the lowest nominal threshold (not including the hysteresis) is at the baseline. With the sub-hysteresis function engaged the nominal threshold can be tuned down to a nominal threshold 9 mV below the baseline. This does not include the hysteresis, which adds approximately 10 mV to the nominal threshold making the threshold approximately 1 mV above the baseline. The PDO is able to read out input amplitudes 56 fC smaller than without for gain=0.5 mV/fC, peaking time=25 ns, and injection capacitance equal to 2.44 pF. The measurements show that for these conditions the VMM1 can measure signal amplitudes 11 mV smaller with the Sub-Hysteresis feature than without.

4. Summary

The first version of the VMM was very successful. The measured performance was well within the predicted simulation. All the features implemented were fully functional. The charge resolution was 0.26 mV at a nominal gain=0.5 mV/fC. The timing resolution was less than 50 ps for a peaking time=25 ns and TAC=125 ns/V. The linearity error of the gain response was less than 0.1%. The Sub-Hysteresis feature enabled the VMM1 to measure signals more than 2 times smaller than without the Sub-Hysteresis. Numerous improvements are planned for the next version, the VMM2. These include improving current features such as the threshold trim range and adding new features such as digitization and more timing outputs.

This manuscript has been authored by employees of Brookhaven Science Associates, LLC under Contract No. DE-AC02-98CH10886 with the U.S. Department of Energy. The publisher by accepting the manuscript for publication acknowledges that the United States Government retains a non-exclusive, paid-up, irrevocable, world-wide license to publish or reproduce the published form of this manuscript, or allow others to do so, for United States Government purposes.

References

[1] T. Alexopoulos, A.A. Altintas, M. Alviggi, M. Arik, S.A. Cetin, V. Chernyatine, E. Cheu, D. Della Volpe, M. Dris, D. Fassouliotis, E.N. Gazis, R. Giordano, V. Gratchev, L. Guan, P. Iengo, P. Ioannou, C. Li, K. Johns, V. Kaushik, A. Khodinov, C. Kourkoumelis, S. Maltezos, K. Mermigka, H. Muller, K. Nikolopoulos, W. Park, S. Persembe, C. Petridou, R. Petti, V. Polychronakos, M.V. Purohit, D. Sampsonidis, G. Sekhniaidze, M. Shao, Y.J. Sun, G. Tsipolitis, R. Veenhof, X.L. Wang, J. Wotschack, S.X. Wu, T. Zhao, Z.G. Zhao, JINST 4 (2009) P12015, http://dx.doi.org/10.1088/1748-0221/4/12/P12015.

[2] G. Tsipolitis, The Muon ATLAS MicroMegas Activity, in: Proc. of Science, 2012 ⟨http://adsabs.harvard.edu/abs/2011ehap.confE.211T⟩.

[3] J. Zhu, The RPC-based proposal for the ATLAS forward muon trigger upgrade in view of super-LHC, in: Proc. of Science, 2012 062 ⟨https://cdsweb.cern.ch/record/1436114⟩.

[4] Y. Giomataris, Ph. Rebourgeard, J.P. Robert, G. Charpak, Nucl. Instrum. Meth. A 376 (1996) 29.

[5] P. Iengo for the MAMMA Collaboration, Development of Micromegas detectors for the upgrade of the ATLAS Muon Spectrometer, Il Nuovo Cimento, ⟨http://www.fe.infn.it/u/fioravanti/Proceeding_IFAE_Divisi_Argomento/LHC/Corretti_Commentati/Iengo_Paolo.pdf⟩.

[6] G. De Geronimo, J. Fried, S. Li, J. Metcalfe, N. Nambiar, E. Vernon, V. Polychronakos, VMM1 - an ASIC for Micropattern Detectors IEEE NSS-MIC, N6-8, October 2012.